Elsevier Editorial System(tm) for
Thermochimica Acta

Manuscript Draft

Manuscript Number:

Title: Structural and DSC Study on Resolution of 2-Methoxy-2-phenylacetic Acid with Chiral 1-Cyclohexylethylamines through Gas-Antisolvent Precipitation

Article Type: Full Length Article

Section/Category: Large volume scanning calorimetry

Keywords: Chiral resolution of S-(+)-O-methylmandelic acid;
Crystal structure determinations by single crystal XRD;
(S)-1-cyclohexylethylammonium (S)-alfa-methoxy-2-phenylacetate salt;
Powder XRD, FTIR spectroscopy and DSC;
Eutectic binary and ternary melting phase diagrams;
Structure-property relationship

Corresponding Author: Dr Janos Madarasz,

Corresponding Author's Institution:

First Author: Amit D Zodge

Order of Authors: Amit D Zodge; Petra Bombicz, Ph.D.; Edit Székely, Ph.D.; György Pokol, Prof. Dr. Ph.D.; Janos Madarasz

Abstract: The system of intermolecular interactions is very similar in the solid state of the chiral and racemic alfa-methoxyphenylacetic acids (alfa-MPAA) indicated by both Differential Scanning Calorimetry (DSC) and FTIR-spectroscopy, and even proved by single crystal structure determination. It makes the resolution of such a racemate challenging even by supercritical fluid extraction. The chiral (S-alfa-methoxyphenylacetic acid (1) crystallizes in orthorhombic crystal system (space group P212121, a = 6.8795(3) Å, b = 7.0124(3) Å, c = 17.4578(8) Å, Z = 4, R = 0.0373), while its 1:1 salt formed with (S)-1-cyclohexylethyl amine (3) is found to be monoclinic (s.g. P21, a = 9.5290(12) Å, b = 6.5909(10) Å, c = 13.869(2) Å, beta = 103.13(3)°, Z = 2, R = 0.0477). The packing arrangement in the (S)-(S) ammonium carboxylate type salt is columnar. The columns are hydrophylic inward and hydrophobic outward, that results in fibrous growth of the salt crystals melting at 163°C. The crystal habit of the higher melting diastereomeric (S)-(R) salt (mp. 187°C) is also fibrous, its structure is closely related to the (S)-(S)-salt by the similarities observed in their FTIR spectra. The DSC and powder XRD studies on the chiral and racemic acids, and on the pair of diastereomeric salts helped us to construct and calculate the binary and ternary phase diagrams of the system components, including their eutectic temperatures and compositions, as well.

Suggested Reviewers: Ludwik Synoradzki Prof. Dr. Ph.D.
Warsaw University of Technology, Faculty of Chemistry
Ludwik.Synoradzki@ch.pw.edu.pl
expert of chiral resolutions

Nikoletta Báthory Ph.D
Cape Peninsula University of Technology
bathorin@cput.ac.za
expert of X-ray crystallography

Alan A Smith Prof. Dr. Ph.D.
ChiRes Ltd, Dudley, UK
aa.smith@virgin.net
master of phase diagram calculations

Cover Letter

Dear Editor,

Please receive our ms entitled as

' Structural and DSC Study on Resolution of 2-Methoxy-2-phenylacetic Acid with Chiral 1-Cyclohexylethylamines through Gas-Antisolvent Precipitation '

by Amit D. Zodge, Petra Bombicz, Edit Székely, György Pokol, and János Madarász

as a submission to Thermochimica Acta.

Sincerely yours

János Madarász

*Manuscript
Click here to view linked References

Manuscript submitted to TCA, 2016. 06. 03.

*Structural and DSC Study on Resolution of 2-Methoxy-2-phenylacetic Acid with Chiral 1-Cyclohexylethylamines through Gas-Antisolvent Precipitation

Amit D. Zodge[a], Petra Bombicz[b], Edit Székely[a], György Pokol,[c] János Madarász[c,*]

[a] Department of Chemical and Environmental Process Engineering, Budapest University of Technology and Economics, HU-1521 Budapest, Hungary. [b] Research Center for Natural Sciences, Hungarian Academy of Science, HU-1117 Budapest, Hungary. [c] Department of Inorganic and Analytical Chemistry, Budapest University of Technology and Economics, HU-1111, Budapest, Hungary.

Abstract

The system of intermolecular interactions is very similar in the solid state of the chiral and racemic α-methoxyphenylacetic acids (α-MPAA) indicated by both Differential Scanning Calorimetry (DSC) and FTIR-spectroscopy, and even proved by single crystal structure determination. It makes the resolution of such a racemate challenging even by supercritical fluid extraction. The chiral (*S*)-α-methoxyphenylacetic acid (**1**) crystallizes in orthorhombic crystal system (space group $P2_12_12_1$, a = 6.8795(3) Å, b = 7.0124(3) Å, c = 17.4578(8) Å, Z = 4, R = 0.0373), while its 1:1 salt formed with (*S*)-1-cyclohexylethyl amine (**3**) is found to be monoclinic (s.g. $P2_1$, a = 9.5290(12) Å, b = 6.5909(10) Å, c = 13.869(2) Å, β = 103.13(3)°, Z = 2, R = 0.0477). The packing arrangement in the (*S*)-(*S*) ammonium carboxylate type salt is columnar. The columns are hydrophylic inward and hydrophobic outward, that results in fibrous growth of the salt crystals melting at 163°C. The crystal habit of the higher melting diastereomeric (*S*)-(*R*) salt (mp. 187°C) is also fibrous, its structure is closely related to the (*S*)-(*S*)-salt by the similarities observed in their FTIR spectra. The DSC and powder XRD studies on the chiral and racemic acids, and on the pair of diastereomeric salts helped us to construct and calculate the binary and ternary phase diagrams of the system components, including their eutectic temperatures and compositions, as well.

Keywords
Chiral resolution; (*S*)-(+)-*O*-methylmandelic acid; crystal structure determinations; (*S*)-1-cyclohexylethylammonium (*S*)-2-methoxy-2-phenylacetate; single crystal and powder X-ray diffraction (XRD); FTIR spectroscopy; Differential Scanning Calorimetry (DSC), binary and ternary melting phase diagrams; eutectic compositions and temperatures; structure-property relationship;

*Corresponding author. Tel.: +36 1 463 4047; fax: +36 1 463 3408.

E-mail address: madarasz@mail.bme.hu (J. Madarász).

1. Introduction

In the last three decades almost one half of the enantiopure drugs are produced by diastereomeric salt formation method using enantiopure resolving agents [1]. Phenylacetic acids and their derivatives are versatile molecules. Several derivatives shows broad range of biological activity, i.e., antibacterial, analgesic, virucidal, plant growth regulator, etc. They are used as important intermediates in the syntheses of their benzamido, phenylacetamido, phenyl benzoxazole derivatives and amino acid esters [1-6].

Chiral forms of 2-methoxy-2-phenylacetic acid (α-MPAA, also called as *O*-methyl mandelic acid) are applied as resolving agents to resolve several racemic amines though diastereomer salt formation [7-11]. Even resolution of racemic 1-cyclohexylethylamine (1-CHEA) was carried out assisted by (*R*)-2-methoxy-2-phenylacetic acid from water and 2-propanol by Sakai et al. [12]. Anyhow Sakai et al. [13] were also able to crystallize both diastereomeric salts of cyclohexylethylamine with (*S*)-mandelic acid, their crystal structures were determined by single crystal X-ray diffraction (CSD [14] reference codes: QEMZEO and QEMZIS, respectively).

Some derivatives prepared from cyclohexylethylamine and cyclodextrins have good separation and binding capacity, which are efficient for chiral acids [15-17] and therefore they are widely used as stationary phase for chiral HPLC columns. The enantiopure 1-cyclohexylethylamines are also used as resolving agents in formation of diastereomeric ester derivatives of various acids. An abundant need for chiral 1-cyclohexylethylamines can be demonstrated with their capability to form chiral salts with certain achiral acids, as well [18-21]. The achiral acid, antracene-2-carboxylic acid, is found to induce a spontaneous resolution of racemic 1-cylcohexylethylamine through formation of salt conglomerate [22].

As a part of our ongoing studies on application of gas-antisolvent method of supercritical CO_2 extraction in resolution systems of various acid-base systems, we collect suitable analytical references to follow resolution of racemic 1-cyclohexylethylamine (1-CHEA) by (*S*)-2-methoxy-2-phenylacetic acid, ((*S*)-α-MPAA). In this way, both racemic and chiral (*S-)* form of α-methoxyphenylacetic acids, as well as both diastereomeric salts formed with the chiral 1-cyclohexylethylamine (1-CHEA) have

been studied (Scheme 1) by differential scanning calorimetry (DSC), FTIR spectroscopy, and powder X-ray diffraction (XRD), in order to explore the various binary and ternary phase relations in the *(R)*- & *(S)*-MPAA - (*R*)-CHEA - system, and its various subsystems. In addition, crystal and molecular structure of the diastereomeric salt (**3**) formed by (*S*)-CHEA and (*S*)-MPAA, along with the parent chiral acid, (*S*)-MPAA have been solved by single crystal X-ray diffraction. Secondary interactions, especially strong H-bonds have been evaluated based on FTIR spectra of the corresponding crystalline *R*-*S* and *S*-*S* salts, as well as on those of chiral and racemic acids, in order to explain the possible driving forces for a successful resolution. Based on DSC-data related eutectic calculations, an overall schematic ternary phase diagram has also been constructed, assembled from partial ones of the various ternary and binary sub-systems, in order to calculate the estimated maximum value of resolubility.

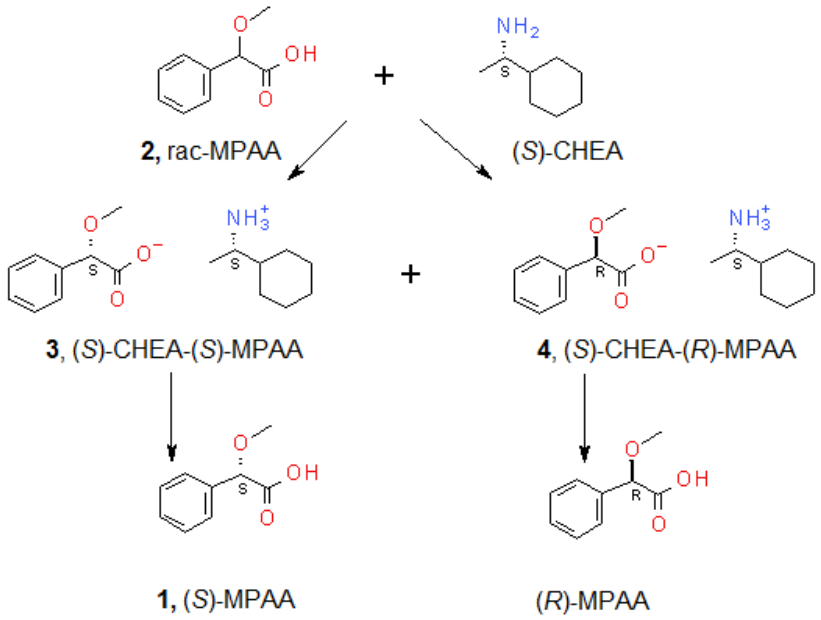

Scheme 1. Scheme of resolution process of racemic α-methoxy-phenylacetic acid with help of chiral (*S*)-1-cyclohexylethylamine as resolving agent

2. Experimental

2.1. Starting materials and sample preparations

The racemic DL-α-methoxyphenylacetic acid (purity > 98%, HPLC) were purchased from TCI Ltd. Belgium [M0837, Lot.WDFNF-SR]. The (*S*) α-methoxyphenylacetic acid

(purity ≥99%, HPLC), 65208-250MG, Lot #BCBB9438V). *R*-(-) and *S*-(+)-1-cyclohexylethylamine (purity > 98%, GC-MS), [727008-1G, Lot # BCBH8287V & [336513-5G Lot #1379720V] respectively purchased from Sigma–Aldrich. CO_2 (99.5 %) was purchased from Linde Gas Hungary Co. (Budapest, Hungary). Methanol, acetonitrile, toluene, 2-propanol and ethanol (> 99 %, GC) was purchased from Merck Ltd. (Darmstadt, Germany).

The transparent single crystals of the diastereomeric salt (**3**) of (*S*)-1-CHEA and (*S*)-α-MPAA were grown by slow evaporation of the solvent mixture from an equimolar solution of toluene-acetonitrile (1 : 1 ratio) (Tol-ACN) at room temperature.

2.1.2 Gas anti-solvent precipitations

The GAS precipitation experiments were carried out in a high-pressure autoclave and briefly discussed in our earlier publication [23]. The reactants (100 ± 0.5 mg (0.60 ± 0.003 mmol) racemic MPAA and 38 ± 0.5mg (0.30 ± 0.03mmol) (*R)*-(-) CHEA) were dissolved separately in 1.5 ± 0.006ml solvent. After complete dissolution the solutions were charged into the thermojaketed autoclave. The autoclave was sealed and filled with CO_2 to the desired pressure followed by 1 hour long stirring for complete precipitation. Before depressurization the reactor was washed with three fold volume (90ml) of sc-CO_2 at the pressure and temperature of the reactor in order to extract the CO_2-soluble components. Extract was trapped in methanol. The solid, crystalline sample recovered from the reactor after depressurization is referred as raffinate. The main component of the extract was non-reacted MPAA whereas raffinate consists of diastereomeric salts.

2.2. Single crystal X-ray diffraction.

A crystal of **1** and **3**, resp. were mounted on a loop. Cell parameters were determined by least-squares using 21630 ($3.13 \leq \theta \leq 27.43°$) reflections for **1**, and using 18600 ($3.02 \leq \theta \leq 27.47°$) reflections for **3**. Intensity data were collected on a Rigaku RAxis Rapid II diffractometer equipped with graphite monochromator [24]. Completeness values are θ = 0.999 (**1**) and θ = 0.996 (**3**). Multi-scan absorption corrections were applied to the data. The structures were solved by direct methods [25]. Anisotropic full-matrix least-squares refinement [25] on F^2 for all non-hydrogen atoms was performed. The weighting scheme

applied was $w = 1/[\sigma^2(F_o^2)+(0.02790.3479P)^2+0.3479P]$ for **1**, while $w = 1/[\sigma^2(F_o^2)+(0.04550.2201P)^2+0.2201P]$ for **3,** where $P = (F_o^2+2F_c^2)/3$. Hydrogen atomic positions were located in difference maps. Hydrogen atoms were included in structure factor calculations but they were not refined. The isotropic displacement parameters of the hydrogen atoms were approximated from the *U*(eq) value of the atom they were bonded to. Crystal data and all other details of the structure determinations and refinements for **1** and **3** are listed in Tables 1, while bond lengths and angles are provided in Supplementary Information File in Tables ST1-ST2 and ST3-ST4, respectively.

Table 1: Summary of crystallographic data, data collection, structure determination and refinement for (*S*)-α-MPAA (1) and (*S*)-CHEA - (*S*)-α-MPAA diastereomeric salt (3).

	(*S*)-α-MPAA (**1**)	(*S*)-CHEA - (*S*)-α-MPAA salt (**3**)
Empirical formula	$C_9H_{10}O_3$	$C_{17}H_{27}NO_3$
Formula weight	166.17	293.39
Temperature	103(2) K	103(2) K
Radiation and wavelength	Mo-Kα, λ =0.71073Å	Mo-Kα, λ =0.71073Å
Crystal system	orthorhombic	monoclinic
Space group	$P2_12_12_1$	$P2_1$
Unit cell dimensions	*a* =6.8795(3)Å	*a* =9.5290(12)Å
	b =7.0124(3)Å	*b* =6.5909(10)Å
	c =17.4578(8)Å	*c* =13.869(2)Å
		β =103.13(3)°
	α =β =γ=90°	α =γ =90°
Volume	842.20(6)Å^3	848.3(2)Å^3
Z, Z`	4, 1	2, 1
Density (calculated)	1.311 Mg/m^3	1.149 Mg/m^3
Absorption coefficient, μ	0.098 mm^{-1}	0.078 mm^{-1}
F(000)	352	320
Crystal colour	Colorless	Colorless
Crystal description	Prism	Prism
Crystal size	0.370 x 0.250 x 0.250 mm	0.550 x 0.150 x 0.100 mm
Absorption correction	Multi-scan	Multi-scan
Max. and min. transmission	0.8952 1.0000	0.4180 1.0000

θ–range for data collection	$3.131 \le \theta \le 27.430°$	$3.016 \le \theta \le 27.483°$
Index ranges	$-8 \le h \le 8;-9 \le k \le 9;-22 \le l \le 22$	$-12 \le h \le 12;-8 \le k \le 8;-18 \le l \le 17$
Reflections collected	28773	32487
Completeness to 2θ	0.999	0.998
Absolute structure parameter	-0.2(3)	1.1(6) *
Friedel coverage	0.681	0.839
Friedel fraction max., full	1.000, 1.000	0.998, 1.000
Independent reflections	1911 [R(int) =0.0513]	3883 [R(int) =0.0863]
Reflections $I>2\sigma(I)$	1776	3504
Refinement method	full-matrix least-squares on F^2	full-matrix least-squares on F^2
Data / restraints / parameters	1911 /0 /114	3883 /1 /193
Goodness-of-fit on F^2	1.109	1.072
Final R indices [$I>2\sigma(I)$]	$R1$ =0.0373, $wR2$ =0.0785	$R1$ =0.0477, $wR2$ =0.1053
R indices (all data)	$R1$ =0.0407, $wR2$ =0.0838	$R1$ =0.0548, $wR2$ =0.1105
Max. and mean shift/esd	0.000;0.000	0.000;0.000
Largest diff. peak and hole	0.175;-0.174 e.Å^{-3}	0.172;-0.196 e.Å^{-3}

*As measured with Mo-Kα radiation and in the lack of heavy atoms showing great anomalous dispersion effect the reliability of the absolute structure parameter is low. The SS conformation is given by experimental evidences.

Crystallographic data for the crystal structures of **1** and **3** have been deposited with the Cambridge Crystallographic Data Centre as supplementary publication number CCDC 1483459 and CCDC 1483460, respectively.

2.3. Further analytical methods (FTIR, XRD, DSC)

FTIR spectra of all the solids were measured by Excalibur Series FTS 3000 (Biorad) FTIR spectrophotometer in KBr between 400 and 4000 cm^{-1}. Powder X-ray diffraction patterns were recorded with a X'pert Pro MDP (PANalytical B.v., The Netherlands) X-ray diffractometer using CuK_α and Ni filter. Differential scanning calorimetry (DSC) measurements were performed using a Modulated DSC 2920 device (TA Instruments, DE, USA). The samples (1-5 mg) were measured in sealed Al-pans at a heating rate of 10 K/min. For temperature and enthalpy calibration of the DSC instrument pure In metal standard was applied.

3. Results

3.1. Crystal structure of (S)-α-MPAA in comparison with the racemic crystal

Single crystal X-ray structure determination of (*S*)-(+)-α-methoxy-2-phenylacetic acid (**1,** Scheme 1) has revealed that it crystallizes in the orthorhombic crystal system, space group $P2_12_12_1$. There is one molecule in the asymmetric unit (Fig. 1a). The angle of the planes of the phenyl and carboxyl groups in **1** is 77.07 °. The absolute configuration of atom C7 is S, the Flack x=-0.2(3) [26]. There is a helical arrangement of the molecules in the crystal lattice along the 'a' crystallographic axis held by the intermolecular hydrogen bond O2-H1…O3 (Table 2, Figure 1b), graph set description is $C^1_1(5)$ [27]. There are weak C2-H2…π intermolecular interactions among the helical columns (Table 2). Polar and apolar layers are formed in the 'ab' crystallographic sheet; they are alternating along the 'c' crystallographic axis (Supplementary Figure SF1).

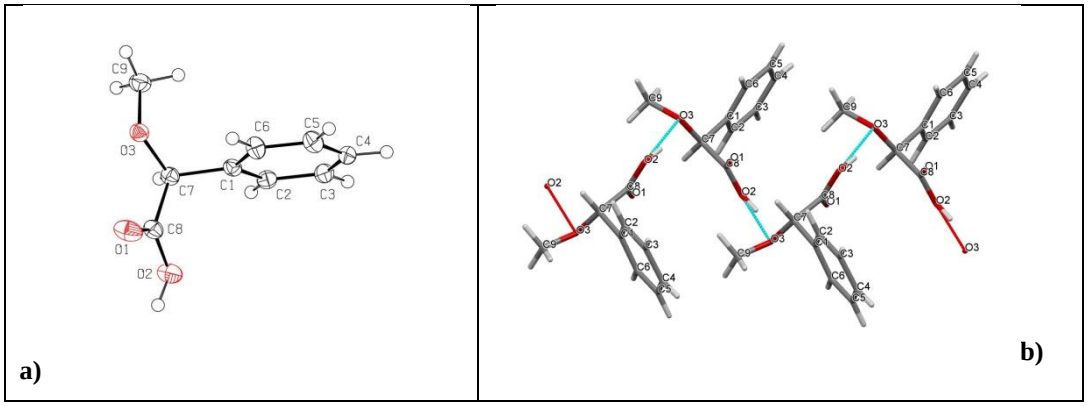

Fig.1. a) Molecular structure [28] of (S)-α-MPAA (**1**). The displacement ellipsoids are drawn at 50% probability level. b) The helical arrangement of molecules along the 'a' crystallographic axis in the crystal lattice of **1** held by OH..O type strong secondary interactions [29].

Table 2. Intermolecular interactions in chiral and racemic crystal form **1** and **2** of acid α-MPAA.

α-MPAA	D-H…A	D-H [Å]	H…A [Å]	D…A [Å]	D-H…A [°]	symm. op.	Ref.
(*S*)-**1**	O2-H1...O3	0.93(4)	1.84(4)	2.749(2)	165(4)	x,-1+y,z	Present work
(*S*)-**1**	C2-H2…π	0.95(4)	2.76	3.649(2)	155	1-x, -1/2+y,1/2-z	Present work
Rac-**2**	O2-H1...O3	0.90(3)	1.85(3)	2.724(3)	162(3)		[30]
Rac-**2**	C4-H4…π	0.99(3)	2.92	3.786(3)	146	1/2-x, 1/2+y,1/2-z	[30]

The crystal structure of the racemic 2-methoxy-2-phenylacetic acid (**2**) (CSD refcode: UNOJOW) was reported in 2004 [30]. **2** crystallizes in the monoclinic crystal system, space group $P2_1/n$. The angle of the planes of the phenyl and carboxyl groups in **2** is 80.80°. The comparison of the molecular conformation of **1** and **2** is shown in Figure 2. The rms of distance differences of the heavy atom positions is 0.6209, the maximum distance difference of atoms is 1.0981 Å. *The chiral columns in **2** assisted by the same kind of OH..O secondary interactions like in **1** are placed in antiparallel arrangement* (Supplementary Figure SF2). A phenyl hydrogen forms C-H…π intermolecular interactions among the helical columns in **2** (Table 2). The phenyl rings do not get close, there is no π...π interaction neither in the crystal lattice of **1** nor in **2**. There are no residual solvent accessible voids in **1** and **2**. The packing coefficient [28] is 69.4% in **1**, what indicates *only a slightly less* efficient packing arrangement compared to the racemic crystal of **2** with 69.7% (Supplementary Figures SF1 and SF2).

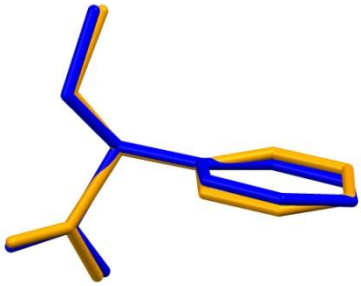

Fig. 2. Comparison of the molecular conformation of the 2-methoxy-2-phenylacetic acid acids from their crystals: **1** (orange) from the (S)-(+)-α- chiral, while **2** (blue) from the racemic crystal.

*3.2. The crystal structure of the diastereomeric salt of (S)-1-CHEA and (S)-α-MPAA (**3**),*

(*S*)-1-Cyclohexylethylammonium (*S*)-α-methoxyphenylacetate **3** (Scheme 1) crystallizes in the monoclinic crystal system, space group $P2_1$. There is one organic salt molecule in the asymmetric unit (Fig. 3a). The angle of the planes of the phenyl and carboxyl groups in **1** is 77.02°, almost like in **1**. The absolute configuration of both chiral centres C7 and C16 is S. The enantiomer has been assigned by reference to a chiral centre which is known from the synthetic procedure. Absolute configuration has not been established by

anomalous-dispersion effects in the diffraction measurement on the crystal **3** in the lack of atoms with high atomic number having strong anomalous dispersion.

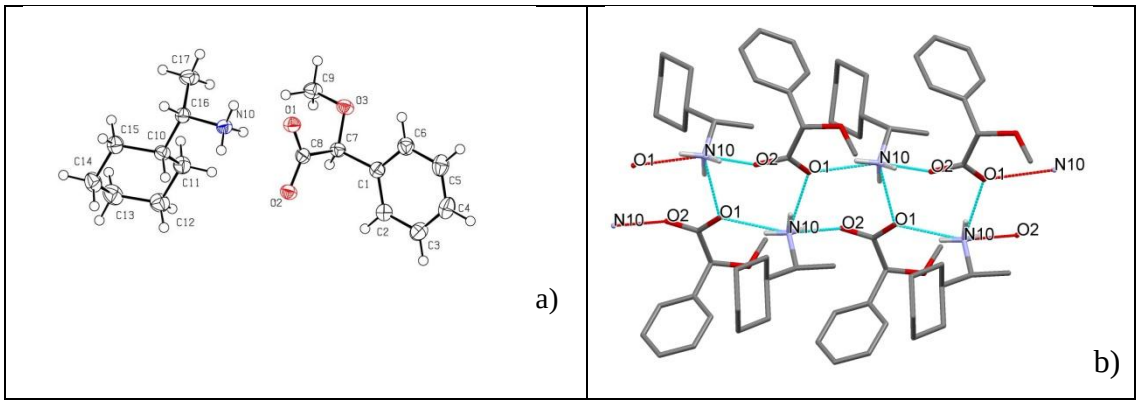

Fig. 3. a) Molecular structure [28] of compound **3**. The displacement ellipsoids are drawn at 50% probability level. b) The ladder type arrangement of the molecules along the 'b' crystallographic axis in the crystal lattice of **3** held by NH…O type strong secondary interactions [29].

Table 3. Intermolecular interactions in *(S)*-1-CHEA-*(S)*-α-MPAA salt **3**.

D-H…A	D-H [Å]	H…A [Å]	D…A [Å]	D-H…A [°]	symm. op.
N10-H10A...O1	0.9100	1.9200	2.782(3)	158.00	intra
N10-H10B...O1	0.9100	1.9500	2.826(3)	162.00	x,1+y,z
N10-H10C...O2	0.9100	1.8900	2.786(3)	170.00	x,1+y,z
C9-H9B...O2	0.9800	2.4400	3.283(3)	143.00	x,1+y,z
C11-H11A...O2	0.9900	2.5500	3.537(3)	175.00	intra

The molecular overlay of the (S)-(+)-α-methoxy-2-phenylacetic acid in **1** and (S)-(+)-α-methoxy-2-phenylacetate moiety in **3** is shown in Figure 4.The placement of the methoxy substituent is different in **1** and **3**, their distance is 1.3964 Å. This alteration of the terminal methyl group makes possible a C9-H9B...O2 interaction in **3** (Table 3) which strengthens the columnar arrangement of the salt along the b crystallographic axis. The strong N-H…O interactions (Table 3, Fig. 3b and Supplementary Fig. SF3) form a ring repeated by the twofold axis described by graph set descriptor [27] as $R^3_4(10)$. *The columns are hydrophilic inward and hydrophobic outward.* There are neither C-H…π nor π...π intermolecular interactions in the crystal of **3**. Potential residual solvent accessible volume is 14.4 $Å^3$ in **3**, it is 1.7% of the unit cell. For comparison a hydrogen bonded water molecule has the expected volume of 40 $Å^3$. The packing coefficient [28] is 66.3% in **3**, the lowest compared with **1** and **2**.

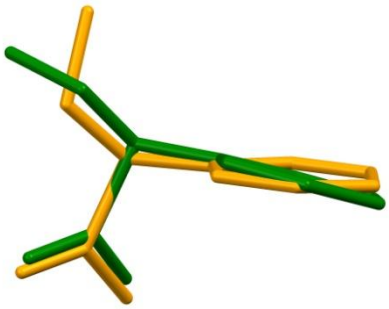

Fig. 4. Comparison of the molecular conformation of *(S)*-α-MPAA acid in **1** (orange) and from *(S)*-1-CHEA-*(S)*-α-MPAA salt **3** (green).

3.3. Characterization of racemic and enantiomeric α-MPAAs, the two diastereomeric salts of α-MPAA and 1-CHEA by FTIR spectroscopy, DSC, and powder XRD.

Results of additional analytical characterization of the four crystalline compounds in the resolution system, i.e. the chiral and racemic α-MPAA acids (**1** and **2**), diastereomeric salt pair with 1-cyclohexylamine, the (*S*)-1-CHEA-(*S*)-α-MPAA (**3**) and (*R*)-1-CHEA-(*S*)-α-MPAA (**4**) salts, are presented comparing their FTIR-spectra (Fig. 5), differential scanning calorimetric curves (DSC, Fig. 6), and powder XRD patterns (Fig. 7).

The overall image of FTIR-spectra of the enantiomeric (*S*-) and racemic α-MPAA acids (**1** and **2**, Fig. 5a and b) are strikingly similar. Their characteristic ν(C=O) carbonyl stretching vibration band is peaked closely at 1755 and 1753 cm^{-1}, the ν(CH) stretching of hydrogen bound to the chiral carbon atom is at 2834 and 2829 cm^{-1}, while free ν(OH) stretching vibration - representing a small portion of OH-groups - is occurring at 3463 and 3456 cm^{-1}, respectively, what show some individual differences, as well. There is a broad absorption band of hydrogen bond system of both forms of acids, starting at lower end of ca. 2500 cm^{-1}, meanwhile there is a difference in its higher limit of wavenumber region (ca. 3600 and 3500 cm^{-1} for **1** and **2**, respectively). The melting points (69.3 and 70.6°C for **1** and **2**, respectively) of acids measured by DSC (Fig. 6a and b) are also very close to each other, the difference between them is almost within the range of experimental errors. These observations have two consequences. Firstly, the two forms of the crystalline acid are hardly distinguishable - at least at the first glances - according to

their FTIR and melting points. To be sure, it is better to take their distinct powder XRD patterns (Fig. 7a and b) to differentiate between them. Secondly, the comparative single crystal structure analysis of the 2-methoxy-2-phenylacetic acid has pointed out the rather similar conformation of the acid molecules adopted in their crystals of **1** and **2**[30]) (Fig. 2), along with their highly similar system of secondary interactions (Table 2). The structural analyses explains the high similarity observed between the vibrations' FTIR spectra, and almost the same extent of lattice stability of the chiral and racemic crystals of α-MPAAs shown by the melting points measured by DSC.

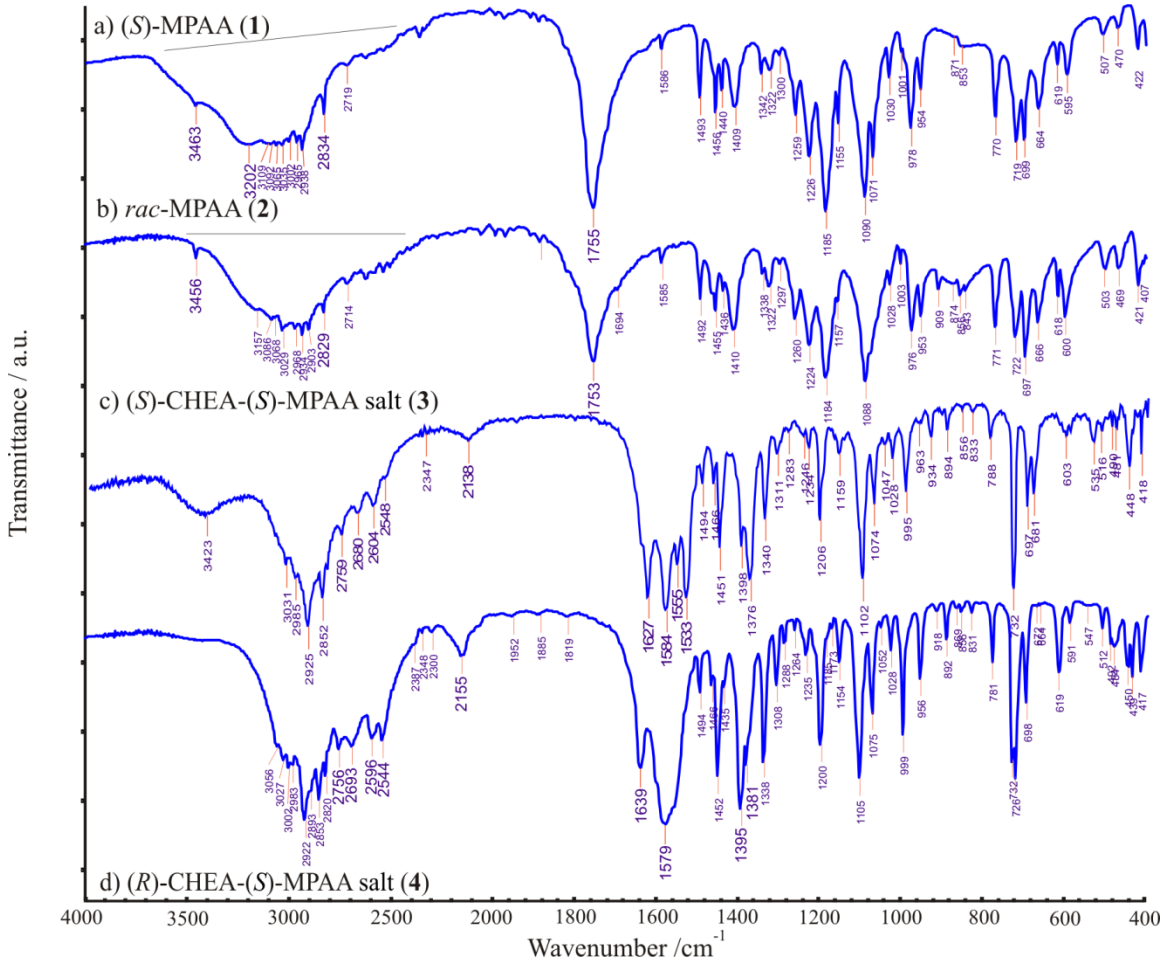

Fig. 5. FTIR spectra of a) enantiomeric (*S*)- (**1**) and b) the racemic α-MPAA (**2**) and the diastereomeric salt pair formed with chiral 1-cyclohexylamine as c) (*S*)-CHEA-(*S*)-MPAA salt (**3**) and d) the corresponding (*R*)-CHEA-(*S*)-MPAA salt (**4**), in comparison.

The FTIR spectra of the corresponding two diastereomeric salts (**3** and **4**) of (S)-α-MPAA with chiral (*S*)- and (*R*)-1-cyclohexylamines resemble also each other (Fig. 5c and d), and show that they both are closely related ammonium salts of a primary amine, as they exhibit a broad medium absorption band in the 2000-2300 cm^{-1} wavenumber region, which represent the strongest part of a hydrogen bond system characteristic for primary ammonium groups, now peaked at $\nu(-NH_3^+)$ = 2138 and 2155 cm^{-1} for (*S*)-1-CHEA-(*S*)-α-MPAA (**3**) and (*R*)-1-CHEA-(*S*)-α-MPAA (**4**) salt, respectively. In case of the (*S*)-(*S*)-salt **3** the single crystal structure analysis proves that the primary ammonium group ($-NH_3^+$) of the (*S*)-1-cyclohexylammonium cation is involved in three N-H…O type hydrogen bonds with oxygen atoms of carboxylate groups of three neighboring (*S*)-O-methylmandelate anions (Fig. 3b) and all the three hydrogen bonds have almost the same short distance between the corresponding donor and acceptor atoms (Table 3). Similarly strong triple hydrogen bonding system can be assumed to exist in the crystal lattice of the other diastereomeric (*R*)-(*S*)-salt **4**, based on similarity of the corresponding IR-absorption band system. Anyhow, the orientational arrangement of the three (*S*)-O-methylmandelate anions around the (*R*)-1-cyclohexylethyl ammonium cation in salt **4** should be different from which occurred in salt **3**, as can be seen from the different intensity and band positions of the symmetric $\nu(COO^-)$ vibration bands of carboxylate anions in the absorption region of 1500-1700 cm^{-1}. There is a kind of IR-reference for salt **4**, as a list of absorption peaks for the mirror salt (*S*)-1-CHEA-(*R*)-α-MPAA (**5**) were published [12]. The peak positions given there are usually with 2-3 cm^{-1} less than those measured now for salt **4**, anyhow they are still within the range allowed by the applied resolution (4 cm^{-1}). Nevertheless there are some bothering exceptions, e.g. the read out of $\nu(-NH_3^+)$ = 2148 cm^{-1} for (**5**), which is out of the error range and in between the values for salts **3** and **4** (Fig. 5c).

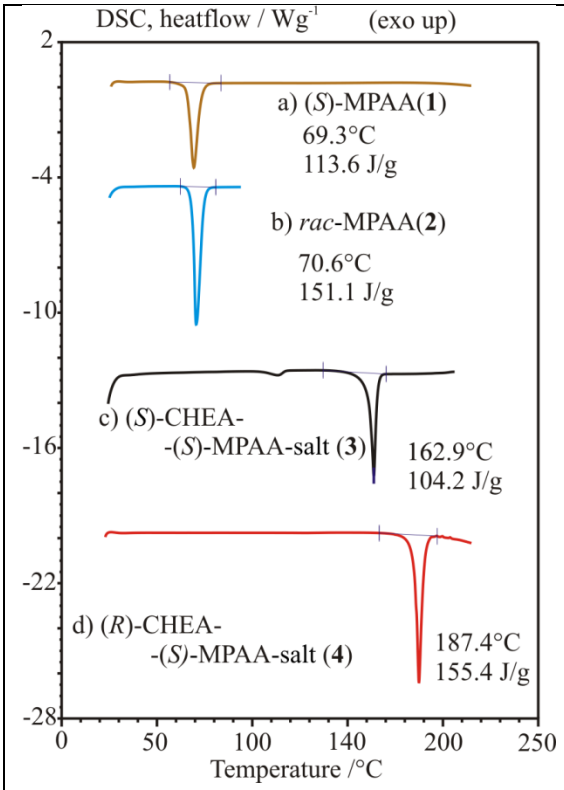

Fig. 6. DSC melting curves of a) (*S*)- and b) racemic α-MPAA (**1** and **2**), and those of two diastereomeric salts (**3** and **4**) formed from c) (*S*)- and d) (*R*)-1-cyclohexylethylamines with (*S*)- α-MPAA, in comparison.

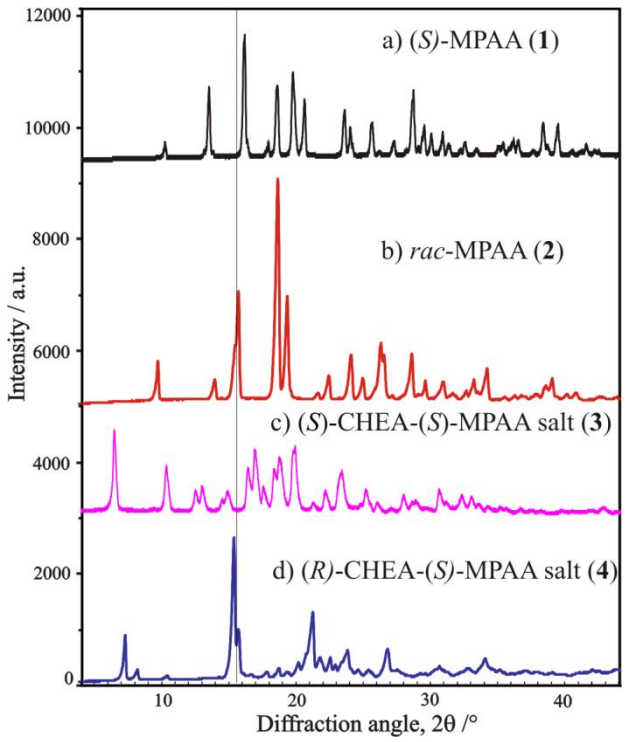

Fig. 7. Powder XRD patterns of a) (*S*)- and b) racemic α-MPAA (**1** and **2**), and those of two diastereomeric salts (**3** and **4**) formed from c) (*S*)- and d) (*R*)-1-cyclohexylethylamines with (*S*)- α-MPAA, in comparison.

DSC analysis of the two diastereomeric salts, (*S*)-1-CHEA-(*S*)-α-MPAA (**3**) and (*R*)-1-CHEA-(*S*)-α-MPAA (**4**), show melting points as 163 and 187°C, respectively (Fig. 6c and d). As reference data, the melting point of salt (*S*)-1-CHEA-(*R*)-α-MPAA (**5**), i.e. mirror salt of **4**) is available only [12], but that mp. is ranging from 178.5 till 180°C, which is actually about 7-8°C lower than that of salt **4** measured by us. Actually no XRD pattern is available for compound **5**, so we cannot decide if salt samples **4** (in our hand) and **5** [12] are in polymorphic relation or we could obtain a purer salt in form of sample **4** (Fig. 7d) compared to salt **5** [12]. All the caloric data on fusion of solid pure samples of **1-4** are listed in Table 4.

Table 4. Melting point and enthalpy of fusion data of the pure chemicals, as applied in this study

Initial chemicals*	T_{fus} observed by DSC K, (°C)	ΔH_{fus} measured by DSC (kJ/mol)	Reference T_{fus} (°C)
(S)-α-MPAA (**1**), applied also for *(R)*-α-MPAA	342.4 (69.3)	18.88	
rac-α-MPAA (**2**)	343.7 (70.6)	50.22 (for S&R formula)	
(*S*)-1-CHEA-(*S*)-α-MPAA (**3**), applied also for its mirror image compound (*R*)-1-CHEA-(*R*)-α-MPAA,	436.0 (162.9)	30.57	-
(*R*)-1-CHEA-(*S*)-α-MPAA (**4**) and its mirror image compound: (*S*)-1-CHEA-(*R*)-α-MPAA (**5**),	460.5 (187.4)	45.59	178.5-180 [12]

* Chemicals listed in the Experimental part were used without further purification, and their experimentally measured parameters were involved into the calculations.

3.4. Eutectic compositions and melting points of the various binary and ternary mixtures in the ternary system of resolution.

Attempts have also been made to study in details the phase relations of the three main basic components, (*S*)-α-MPAA, (*R*)-α-MPAA, and (*R*)-1-CHEA, in order to support the resolution of racemic α-MPAA with chiral 1-CHEA. Actually, we decided to establish all of the melting phase diagram of the binary and ternary eutectic subsystems observed including solids (*S*)-α-MPAA (**1**), *rac*-α-MPAA (**2**), (*R*)-1-CHEA-(*S*)-α-MPAA (**4**) and (*S*)-1-CHEA-(*S*)-α-MPAA (**3**), (the latter compound was prepared and applied instead of its mirror image compound (*R*)-1-CHEA-(*R*)-α-MPAA, because of the lack of initial pure sample of (*R*)-α-MPAA available), based on experimentally measured melting point and enthalpy of fusion of solid compounds **1-4**, measured and summarized in Table 4.

First, estimation of each eutectic molar fraction, eutectic temperature, and liquidus curves of binary eutectic phase diagrams have been calculated numerically [31, 32] based on the temperature and enthalpy of fusion of pure crystalline phases (listed in Table 4) assuming the validity of simplified Schröder-van Laar equation, and in case of

racemate also of Prigogine-Defay-Mauser equation [33]. The solid-liquid melting phase diagram for mixtures of (*S*)-α-MPAA and (*R*)-α-MPAA was formerly investigated by Raznikiewicz [34], where this binary system resembled also a type of melting phase diagram including a racemic compound, which showed higher melting point than the enantiomers (ibid).

Table 5: Calculated eutectic compositions and eutectic temperatures of binary and ternary mixtures (based on experimental DSC data of used and prepared chemicals and assumption of validity of Schöder-van Laar equation).

Components	Calculated eutectic molar fractions, x_{eu}	Calculated eutectic temperature T_{eu} (K, °C)
(*S*)-α-MPAA (**1**) (or (*R*)-α-MPAA) / *rac*-α-MPAA (**2**)	$x_{(\boldsymbol{S}\text{-}\mathbf{1})} = 0.658$ $x_{(\mathbf{rac}\text{-}\mathbf{2})} = 0.342$	333, 60 Prigogine-Defay equation also applied
(*S*)-α-MPAA (**1**)/ (*R*)-1-CHEA-(*S*)-α-MPAA (**4**)	$x_{(\boldsymbol{S}\text{-}\mathbf{1})} = 0.984$ $x_{(\boldsymbol{RS}\text{-}\mathbf{4})} = 0.016$	341.5, 68.5
rac-α-MPAA (**1**)/ (*R*)-1-CHEA-(*S*)-α-MPAA (**4**)	$x_{(\mathbf{rac}\text{-}\mathbf{2})} = 0.983$ $x_{(\boldsymbol{RS}\text{-}\mathbf{4})} = 0.017$	343, 70
(*S*)-α-MPAA (**1**)/ *rac*-α-MPAA (**2**)/ (*R*)-1-CHEA-(*S*)-α-MPAA (**4**)	$x_{(\boldsymbol{S}\text{-}\mathbf{1})} = 0.671$ $x_{(\mathbf{rac}\text{-}\mathbf{2})} = 0.323$ $x_{(\boldsymbol{RS}\text{-}\mathbf{4})} = 0.006$	323, 50
(*R*)-α-MPAA / (*R*)-1-CHEA-(*R*)-α-MPAA Substituted by as its mirror image: (*S*)-α-MPAA(**1**)/ (*S*)-1-CHEA-(*S*)-α-MPAA (**3**)	$x_{(\boldsymbol{R})} = 0.914$ $x_{(\boldsymbol{RR})} = 0.086$ considered as same as $x_{(\boldsymbol{S}\text{-}\mathbf{1})} = 0.914$ $x_{(\boldsymbol{SS}\text{-}\mathbf{3})} = 0.086$	338, 65
rac-α-MPAA (**2**)/ (*R*)-1-CHEA-(*R*)-α-MPAA or (*S*)-1-CHEA-(*S*)-α-MPAA (**3**)	$x_{(\boldsymbol{rac}\text{-}\boldsymbol{2})} = 0.906$ $x_{(\boldsymbol{RR})} = 0.094$	342, 69
(*R*)-α-MPAA / *rac*-α-MPAA (**2**)/ (*R*)-1-CHEA-(*R*)-α-MPAA Substituted by as its mirror image: (*S*)-α-MPAA(**1**)/ *rac*-α-MPAA (**2**)/ (*S*)-1-CHEA-(*S*)-α-MPAA (**3**)	$x_{(\boldsymbol{R})} = 0.651$ $x_{(\mathbf{rac}\text{-}\mathbf{2})} = 0.299$ $x_{(\boldsymbol{RR})} = 0.050$ considered as same as $x_{(\boldsymbol{S}\text{-}\mathbf{1})} = 0.651$ $x_{(\boldsymbol{rac}\text{-}\boldsymbol{2})} = 0.299$ $x_{(\boldsymbol{SS}\text{-}\mathbf{3})} = 0.050$	321.5, 48.5
(*R*)-1-CHEA-(*S*)-α-MPAA (**4**)/ (*R*)-1-CHEA-(*R*)-α-MPAA or (*S*)-1-CHEA-(*S*)-α-MPAA (**3**)	$x_{(\boldsymbol{RS}\text{-}\mathbf{4})} = 0.300$ $x_{(\boldsymbol{RR})} = 0.700$	418, 145
rac-α-MPAA (**2**)/ (*R*)-1-CHEA-(*S*)-α-MPAA (**4**)/ (*R*)-1-CHEA-(*R*)-α-MPAA or (*S*)-1-CHEA-(*S*)-α-MPAA (**3**)	$x_{(\boldsymbol{rac}\text{-}\boldsymbol{2})} = 0.888$ $x_{(\boldsymbol{RS}\text{-}\mathbf{4})} = 0.015$ $x_{(\boldsymbol{RR})} = 0.097$	341.5, 68.5

Beyond the results on various binary subsystems, the calculated eutectic parameters for ternary eutectic subsystems, according to the Schröder-van Laar equation [35-37] are also calculated and reported in Table 5. A schematic diagram of overall phase relation of the three-component ((*S*)-α-MPAA, (*R*)-α-MPAA, and (*R*)-1-CHEA) system, that allows the required resolution, is exhibited in Fig. 8.

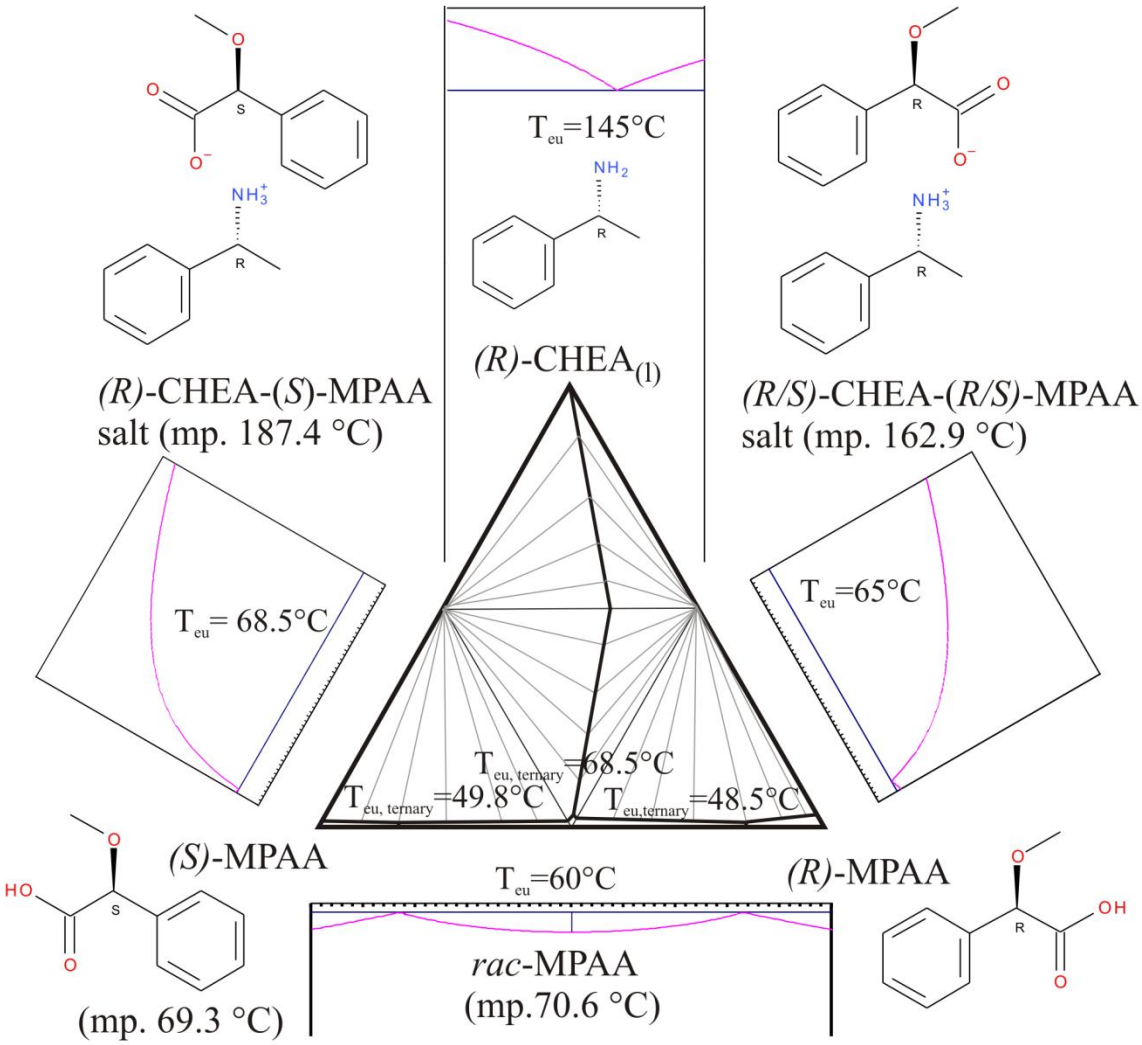

Fig. 8. Schematic three-component T–x phase diagram for α-methoxyphenylacetic acids and (*R*)-1-cyclohexylethylamine, drawn from the data summarized in Table 5. Schematic T–x diagrams for several pair of components (including that of the pair of diastereomeric salts, at the top) are also shown.

The large differences between the melting points of the acidic forms (that of either racemate or chiral one) and the diastereomeric salts (those of either homochiral (*S*)-(*S*)- or (*R*)-(*R*)- or heterochiral (*R*)-(*S*)- or (*S*)-(*R*)- ones), which are greater than 95°C, indicates that one of the diastereomeric salt forms will precipitate first from any mixed solution of racemic α-MPAA acid with chiral 1-CHEA amine. The difference between the solubility of the homochiral and heterochiral salts seems to be not too large, as can be judged from their melting point difference of ca. 21°C. A predicted maximal efficiency of resolution, the so called resolvability (S, or Fogassy parameter) can be calculated according to the following equation: $S=(1-2x_{eu})/(1-x_{eu})$, where x_{eu} is the molar fraction of diastereomeric salt with the higher melting point in the binary system of pair of the diastereomeric salts, which are in eutectic solid phase relation (forming conglomerates of the two salt crystals). In our case, the diastereomeric salts' eutectic molar composition is calculated as $x_{R\text{-}S,\ eu} = 0.342$ (Table 5), and resolvability parameter is determined by a value of S = 0.48 for the maximum efficiency of resolution available in the ternary system of acids and the given resolving chiral amine.

Conclusions

Close melting points and high similarity in FTIR spectra of racemic and enantiopure (*R*)-α-methoxyphenylacetic acids indicated that several other physical properties and the internal structural forces may be rather similar in the two solid forms. It has been proven by comparison the molecular conformations and hydrogen bonding systems of the acid molecules in crystalline racemate (**1**), determined newly by single crystal X-ray diffraction and those of chiral acid (**2**), already known from the literature.

The FTIR spectra of diastereomeric salts (**3** and **4**) have also been found rather similar, indicating similarity in systems of secondary interactions in their solid structures. Single crystal could be grown from (*S*)-1-CHEA-(*S*)-α-MPAA (**3**) only, therefore merely implications could be drawn on the hydrogen bonding system of the salt (*S*)-1-CHEA-(*R*)-α-MPAA (**4**) of higher melting point (187°C). In **4,** all three hydrogen atoms of the primary ammonium anion also take place in three stronger hydrogen bonds, as it has been proven in case of salt **3**. This implication is also an important one, as salt **4** has been

always found as firstly precipitated solid component in various resolution trials of ours carried out in supercritical fluid (CO_2) resolution in presence of excess acids.

The various binary phase relations in the ternary resolution system of main components have been studied by differential scanning calorimetry (DSC) and powder X-ray diffraction (XRD). Based on related eutectic calculations, a schematic ternary phase diagram has been constructed, as well the maximum of the available resolution efficiency has been estimated with a Fogassy's parameter value of S = 0.48.

Acknowledgements

This work was performed within the Marie Curie early stage researcher DoHip Network, a project within the European Community's Seventh Framework Programme (FP7/2013-2016) under grant agreement No. 316959, and Hungarian Scientific Research Fund's grant Nos. OTKA K-100801 and OTKA K-108979, which are gratefully acknowledged. E.Sz. thanks the support of János Bolyai Research Fund of the Hungarian Academy of Science.

Supplementary material

Additional crystallographic information available in form of figures and tables (Supplementary Figs. SF1-3 and Tables ST1-4) in one file.

References

[1] Rouhi AM., Chiral Bus. (2003) 81(18): 45–55.

[2] K.M. Takashi O. Eiji T, Kanae D, Mifune T, Synlett (2000) 2000(10): 1500-1502

[3] N.C. Tuncel G, Lett. Appl. Microbiol 17 (1993) 300-302

[4] Alan N., Duncan Bruce J., Brown D.S., Eur. Pat. Appl. Ep 343,900 (Cl. Co7D241/04)

[5] E.A. Şener, Ö. Temiz Arpacı, İ. Yalçın, N. Altanlar, Farm. 55 (2000) 397–405.

[6] M. Kasthuri, C. El Amri, V. Lefort, C. Perigaud, S. Peyrottes, New J. Chem. 38 (2014) 4736–4742.

[7] US Patent Application No. US2006/063943A1, Inventors: K. Sakai, R. Sakurai, A. Yuzawa, K. Hatahira. Applicant: Yamakawa Chemical Co., Ltd., (Example No. 3).

[8] European Patent Application No. EP2168943A1, Inventors: R. Ogawa, T. Fujino, K. Sakai, Applicant: Toray Finechemicals Co., Ltd., (Examples No. 1-6).

[9] J. Touet, L. Faveriel, E Brown, Tetrahedron, 51 (1995) 1709-1720.

[10] R. Sakurai, A. Yuzawa, K. Sakai, Tetrahedron: Asymmetry, 19 (2008) 1622–1625.

[11] K. Tomooka, M. Suzuki, M. Shimada, S. Yanagitsuru, K. Uehara, Org. Lett., 8 (2006) 963-965.

[12] K. Sakai, M. Yokoyama, R. Sakurai, N. Hirayama, Tetrahedron: Asymmetry, 17 (2006) 1541-1543.

[13] K. Sakai, R. Sakurai, N. Hirayama, Tetrahedron: Asymmetry, 17 (2006) 1812-1816.

[14] F.H. Allen. Acta Cryst. B 58 (2002) 380-388.

[15] S. V Kurkov, T. Loftsson, Int. J. Pharm. 453 (2013) 167–80.

[16] E.M.M. Del Valle, Process Biochem. 39 (2004) 1033–1046.

[17] L. Escuder-Gilabert, Y. Martín-Biosca, M.J. Medina-Hernández, S. Sagrado, J. Chromatogr. A 1357 (2014) 2–23.

[18] S. Nagahama, K. Inoue, K. Sada, M. Miyata, A. Matsumoto, Cryst.Growth Des. 3 (2003) 247-256, [CSD ref. code ASONOL.]

[19] S. Chen, B. O. Patrick, J. R. Scheffer, J. Org. Chem. 69 (2004) 2711-2718, [CSD ref. code AXOXOA.]

[20] I. Turowska-Tyrk, J. Bakowicz, J. R. Scheffer, W.Xia, CrystEngComm., 8 (2006) 616-621, [CSD ref.codes LICRUL01-LICRUL11.]

[21] M. Botoshansky, D. Braga, M. Kaftory, L. Maini, B. O. Patrick, J. R. Scheffer, K. Wang, Tetrahedron Lett., 46 (2005) 1141-1144, [CSD ref.codes YAHTOR and YAHTUX.]

[22] Y.Imai, K.Kamon, K.Murata, T.Harada, Y.Nakano, T.Sato, M.Fujiki, R.Kuroda, Y.Matsubara Org. Biomol. Chem.,6 (2008) 3471-3475, [CSD ref.code QOGNEG]

[23] A. Zodge, M. Kőrösi, M. Tárkányi, J. Madarász, I. M. Szilágyi, T. Sohajda, E. Székely, Can. J. Chem. Eng., submitted.

[24] CrystalClear SM 1.4.0 (Rigaku/MSC Inc., 2008).

[25] G. M. Sheldrick, 25, Acta Cryst. A64 (2008) 112-122.

[26] H. D. Flack Acta Cryst. A39 (1983) 876-881.

[27] J. Grell, Bernstein, G. Tinhofer: Crystallogr. B: Struct. Sci. 56 (2000) 166

[28] A. L. Spek, J.Appl.Cryst. 2003, 36, 7-13.

[29] C. F. Macrae, P. R. Edgington, P. McCabe, E. Pidcock, G. P. Shields, R. Taylor, M. Towler and J. van de Streek J. Appl. Cryst, 39, 453-457, 2006

[30] J. Hartung, K. Spehar, I. Svoboda, H.Fuess, Acta Crystallogr., Sect.E: Struct. Rep. Online (2004), 60, o95, doi:10.1107/S1600536803028228.

[31] D. Kozma, G. Pokol, M. Ács, J. Chem. Soc., Perkin Trans. 2 (1992) 435.

[32] J. Madarász, D. Kozma, G. Pokol, M. Ács, E. Fogassy, J. Therm. Anal. Calorim. 42 (1994) 877-894.

[33] J. Jacques, A. Collet, S. H. Wilen, Enantiomers, racemates, and resolution, John Wiley & Sons, New York, 1981.

[34] T. Raznikiewicz, Acta Chem. Scand. 16 (1962) 1097-1102

[35] A. A. Smith, Tetrahedron: Asymmetry 9 (1998) 2925-2937.

[36] P. Thorey, P. Bombicz, I. M. Szilágyi, P. Molnár, G. Bánsághi, E. Székely, B. Simándi, L. Párkányi, G. Pokol, J. Madarász, Thermochim. Acta 497 (2010) 129–136, and refs therein.

[37] Z. Szeleczky, E. Kis-Mihály, S. Semsey, H. Pataki, P. Bagi, E. Pálovics, G. Maros, G. Pokol, E. Fogassy, J. Madarász, Ultrason. Sonochem. 32 (2016) 8-17.

Legends for Figures

Scheme 1. Scheme of of resolution process of racemic α-methoxy-phenylacetic acid with help of chiral (S)-1-cyclohexylethylamine as resolving agent

Fig. 1. a) Molecular structure of (S)-α-MPAA (compound **1)** [28]. The displacement ellipsoids are drawn at the 50% probability level. b) The helical arrangement of molecules along the 'a' crystallographic axis in the crystal lattice of **1** [29] held by OH..O type strong secondary interactions.

Fig. 2. Comparison of the molecular conformation of acids in crystals of chiral **1** (orange) and racemic **2** (blue).

Fig. 3. a) Molecular structure of compound **3** [28]. The displacement ellipsoids are drawn at the 50% probability level. b) The ladder type arrangement of molecules along the 'b' crystallographic axis in the crystal lattice of 3 [29] held by NH..O type strong secondary interactions.

Fig. 4. Comparison of the molecular conformation of *(S)*-α-MPAA acid in **1** (orange) and *(S)*-1-CHEA-*(S)*-α-MPAA salt **3** (green).

Fig. 5. FTIR spectra of a) the racemic (**2**) and b) enantiomeric (S)-α-MPAA (**1**) and the diastereomeric salt pair formed with chiral 1-cyclohexylamine as c) (*S*)-CHEA-(*S*)-MPAA salt (**3**) and d) the corresponding (*R*)-CHEA-(*S*)-MPAA salt (**4**), in comparison.

Fig. 6. DSC melting curves of a) (*S*)- and b) racemic α-MPAA (**1** and **2**), and those of two diastereomeric salts (**3** and **4**) formed from c) (*S*)- and d) (*R*)-1-cyclohexylethylamines with (*S*)-α-MPAA, in comparison.

Fig. 7. Powder XRD patterns of a) (*S*)- and b) racemic α-MPAA (**1** and **2**), and those of two diastereomeric salts (**3** and **4**) formed from c) (*S*)- and d) (*R*)-1-cyclohexylethylamines with (*S*)-α-MPAA, in comparison.

Fig. 8**.** Schematic three-component T–x phase diagram for α-methoxyphenylacetic acids and (*R*)-1-cyclohexylethylamine, drawn from the data summarized in Table 5. Schematic T–x diagrams for each pair of components (including that of the pair of diastereomeric salts, at the top) are also shown.

Legend for Tables

Table 1: Summary of crystallographic data, data collections, structure determination and refinement for (*S*)-α-MPAA (**1**) and (*S*)-CHEA - (*S*)-α-MPAA diastereomeric salt (**3**).

Table 2. Intermolecular interactions in chiral and racemic crystal form **1** and **2** of acid α-MPAA.

Table 3. Intermolecular interactions in *(S)*-1-CHEA-*(S)*-α-MPAA salt **3**.

Table 4. Melting point and enthalpy of fusion data of the pure chemicals, as applied in this study.

Table 5: Calculated eutectic compositions and eutectic temperatures of binary and ternary mixtures (based on experimental DSC data of used and prepared chemicals and assumption of validity of Schöder-van Laar equation).

List of Supplementary Figures and Tables

Scheme 1

Click here to download high resolution image

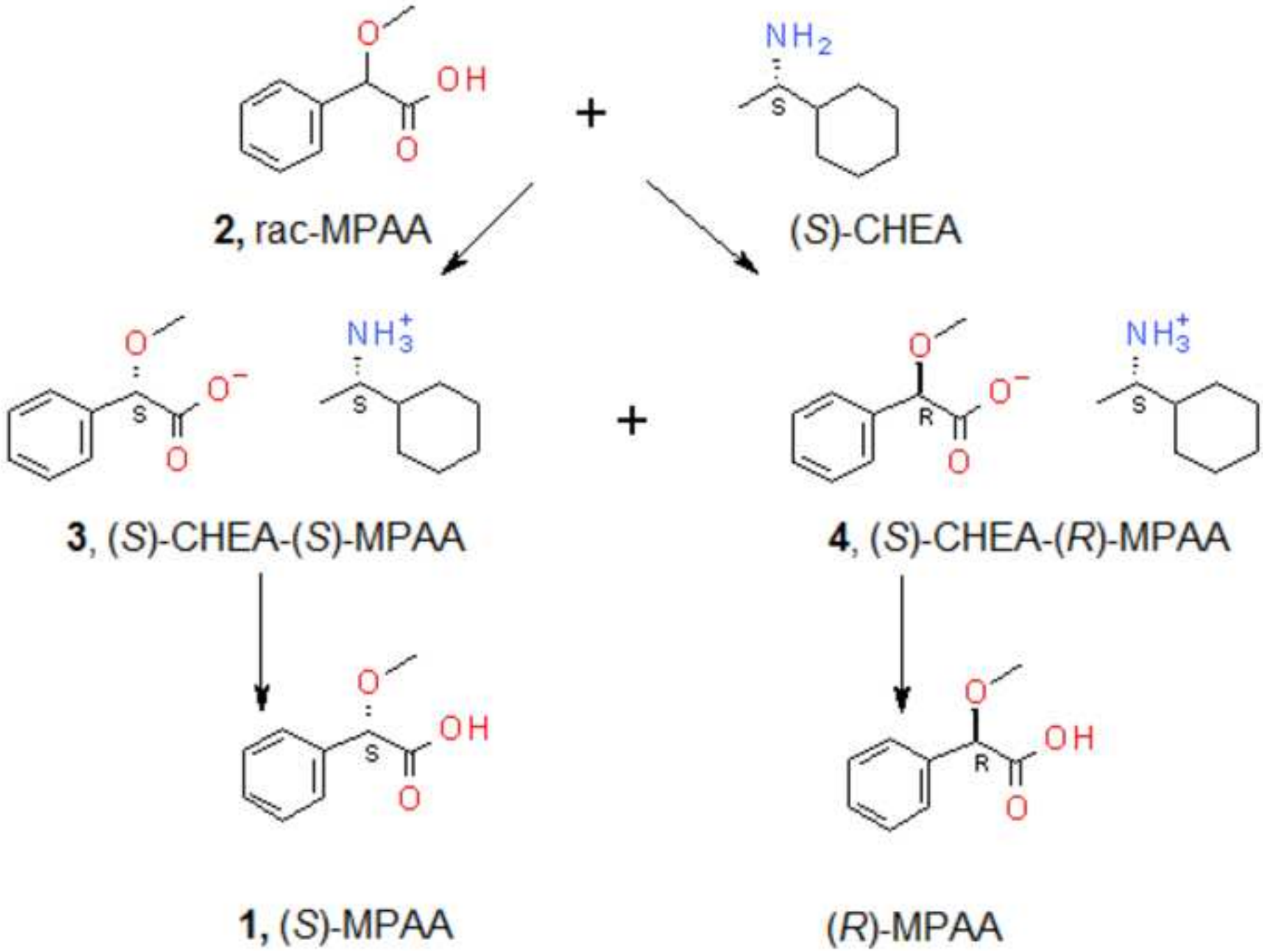

Figure 1a

Click here to download high resolution image

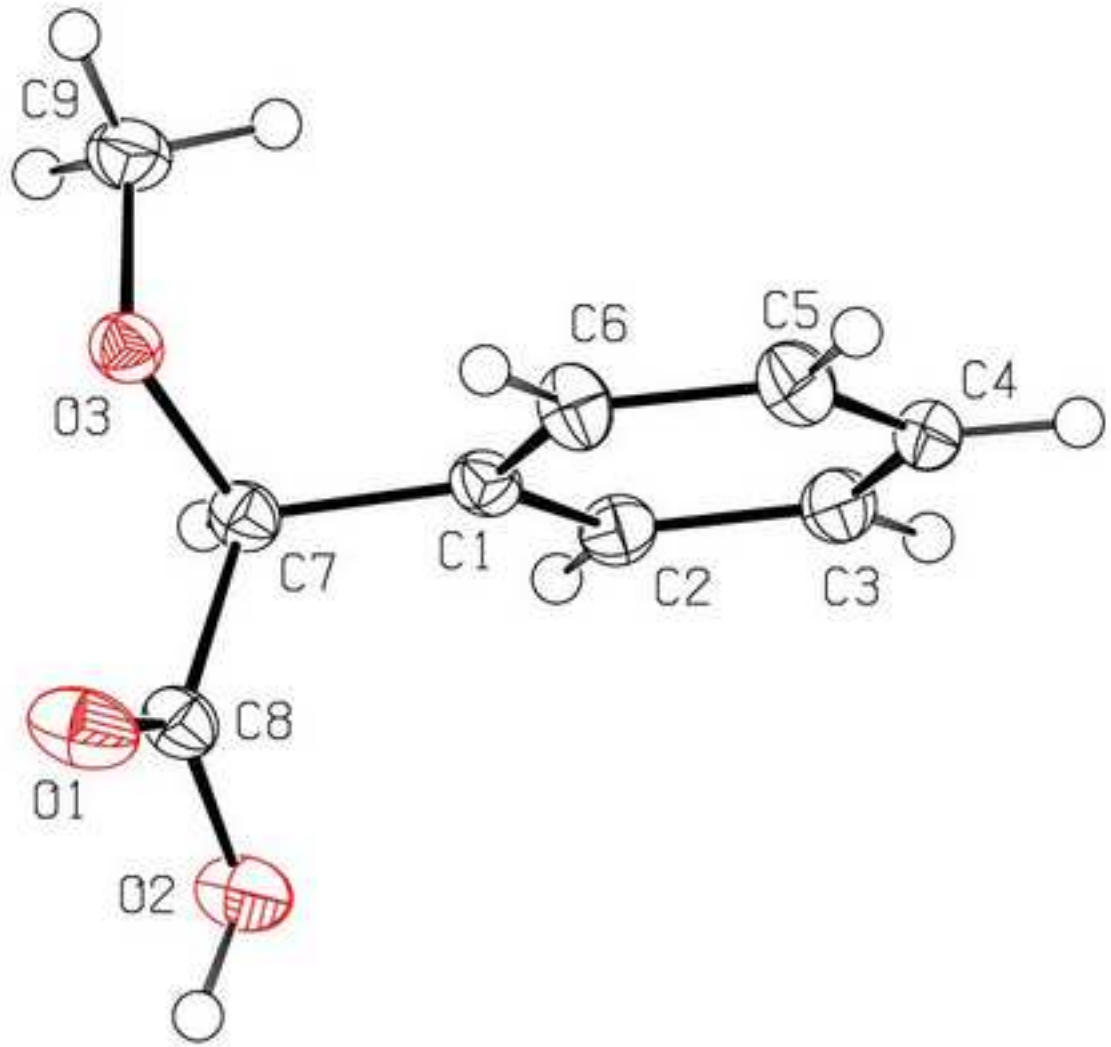

Figure 1b

Click here to download high resolution image

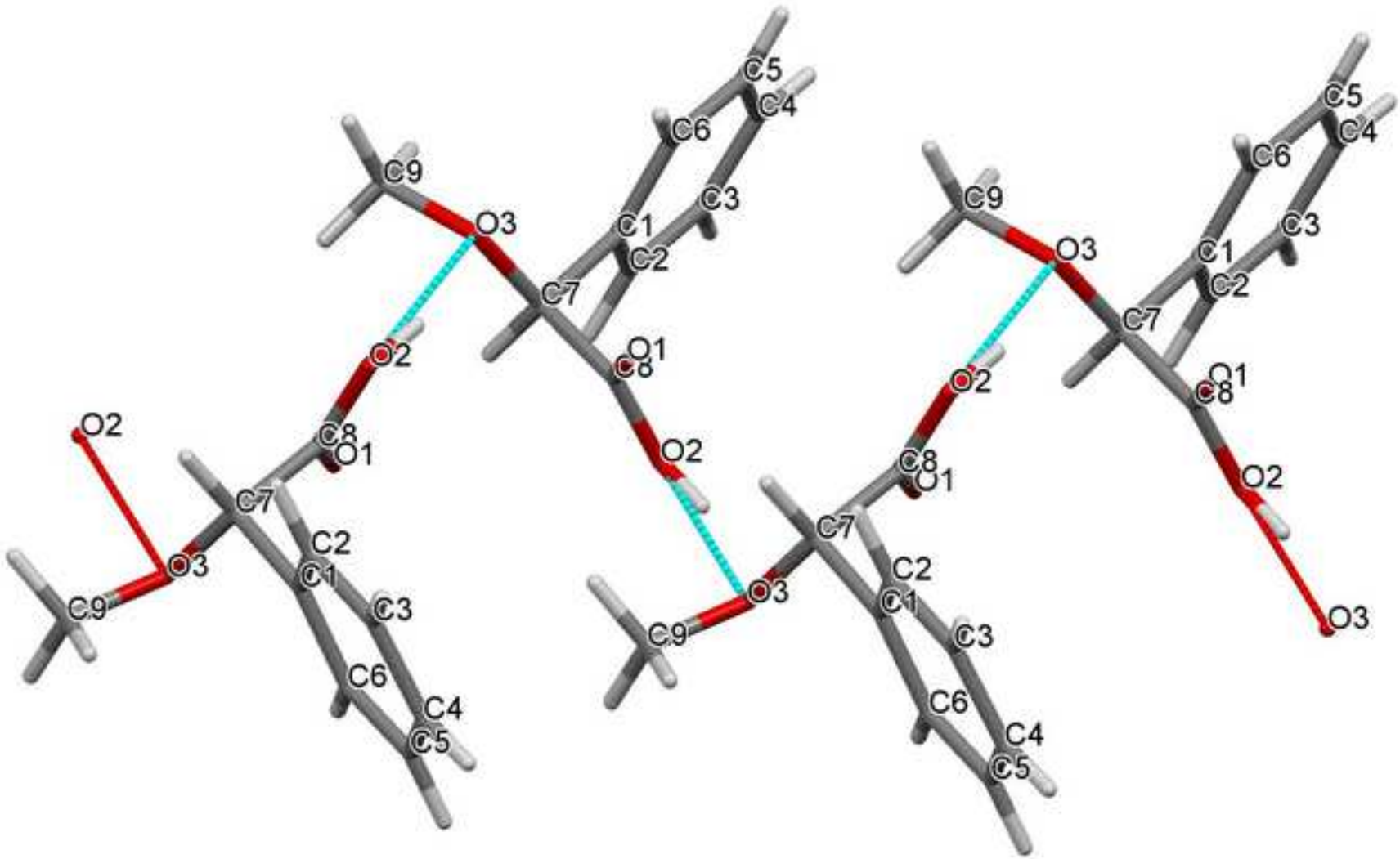

Figure 2

Click here to download high resolution image

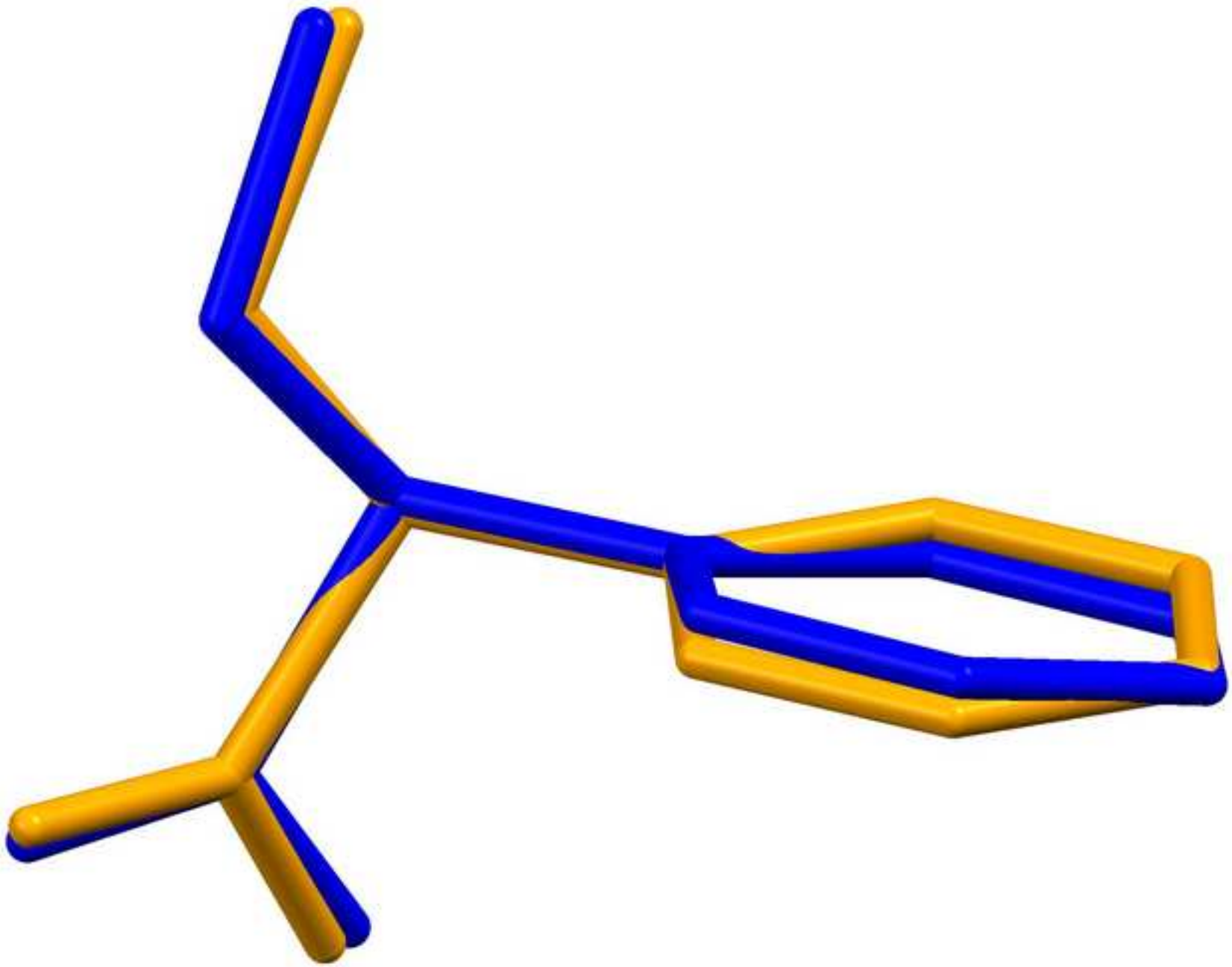

Figure 3a

Click here to download high resolution image

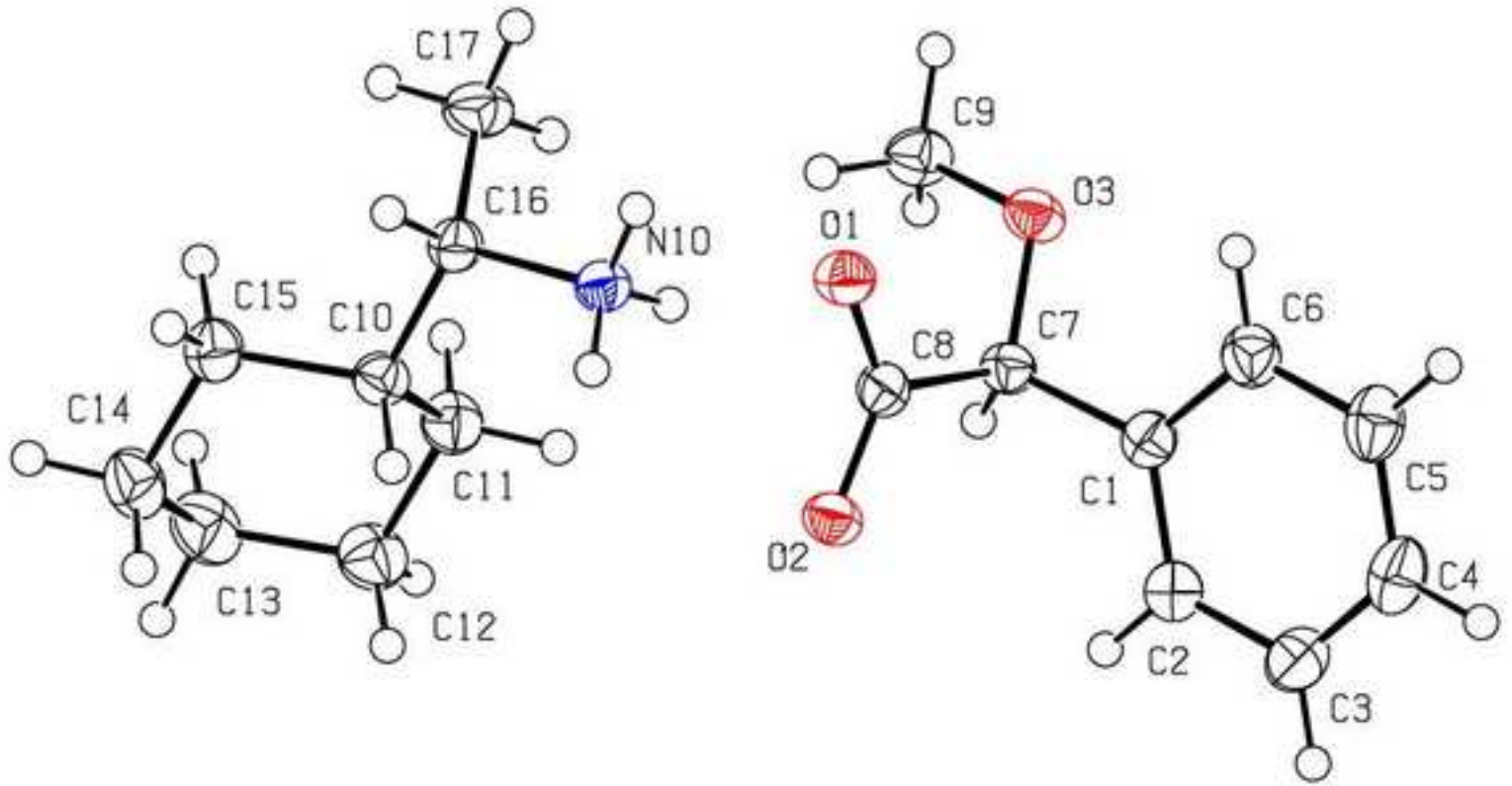

Figure 3b

Click here to download high resolution image

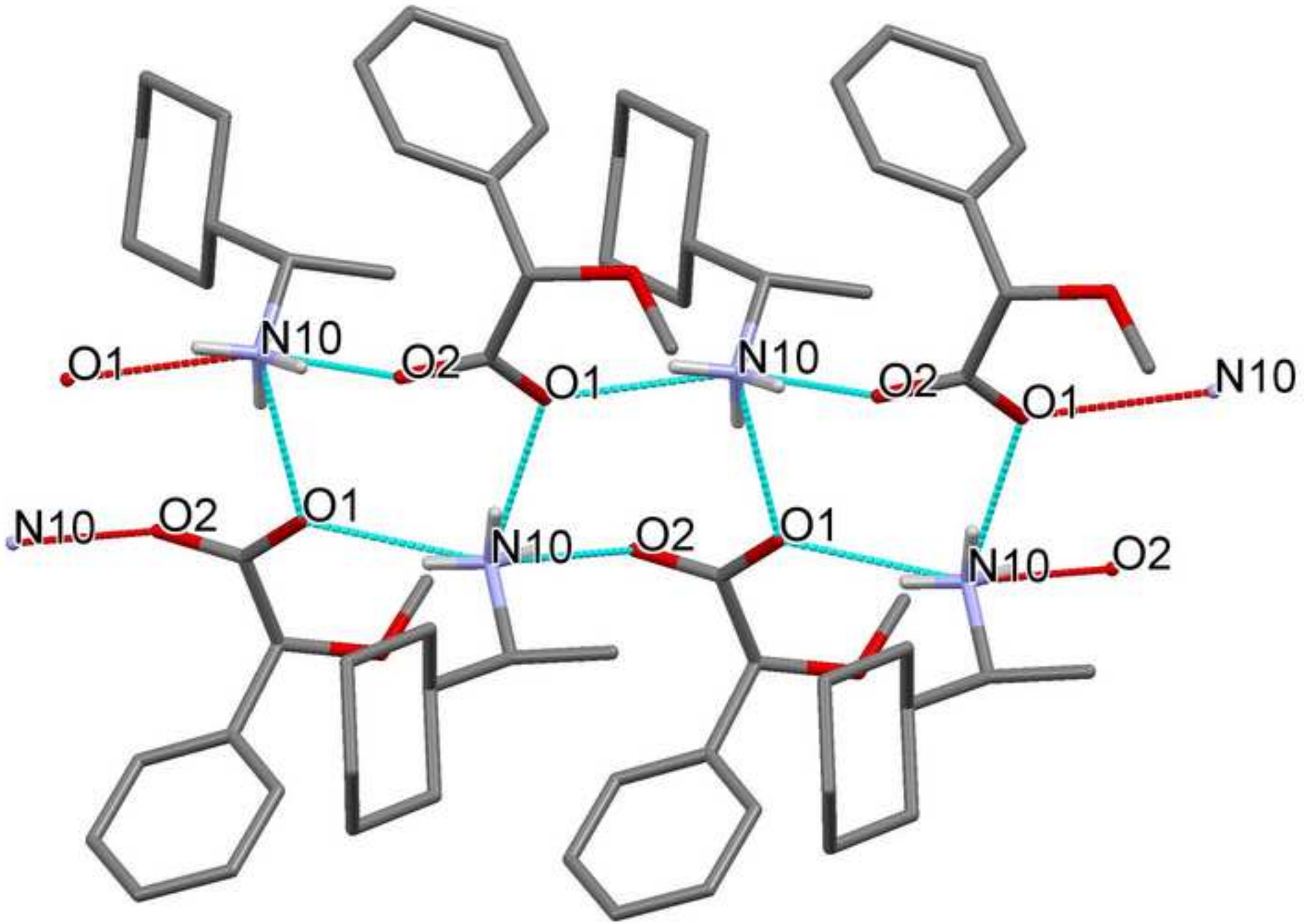

Figure 4

Click here to download high resolution image

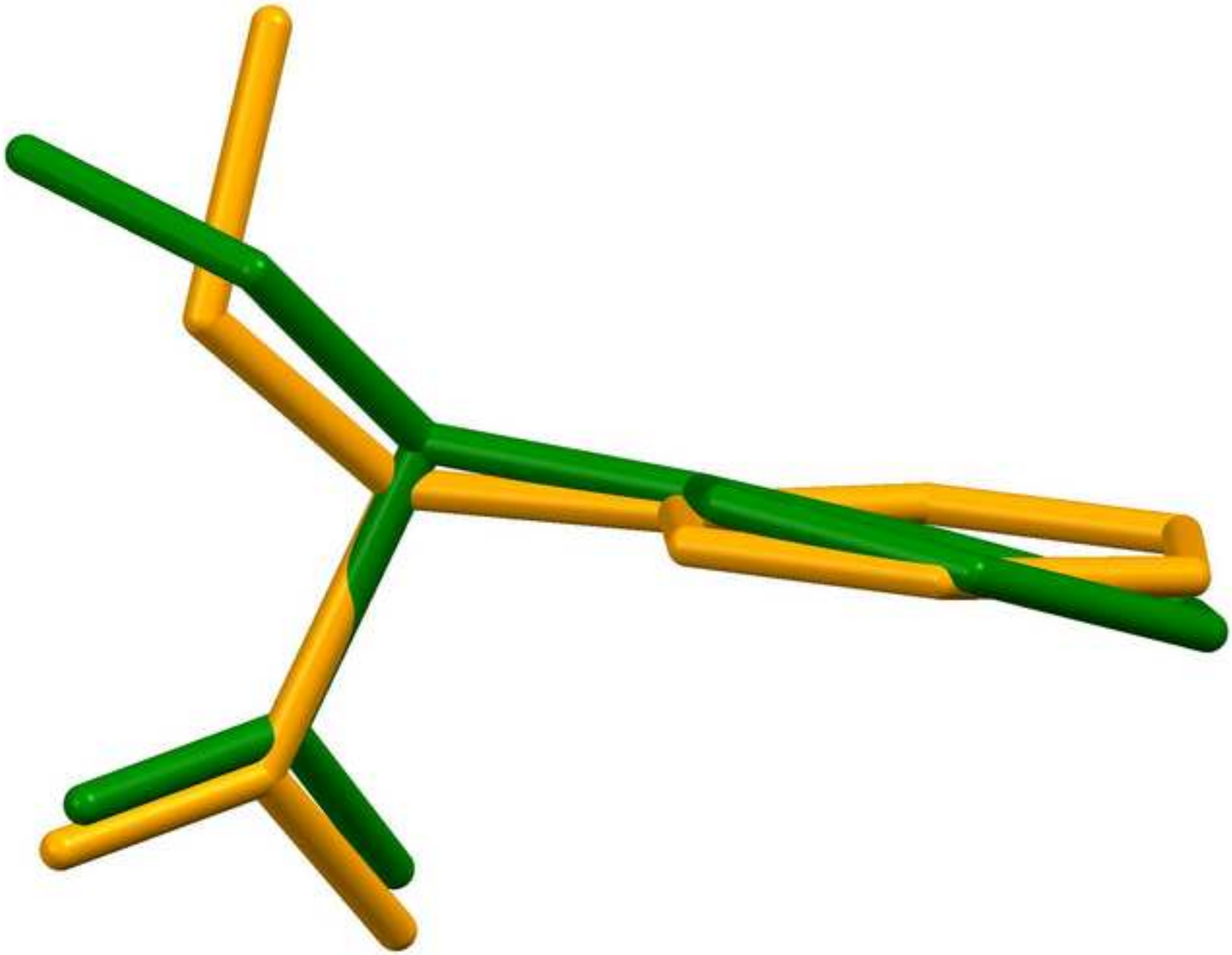

Figure 5

Click here to download high resolution image

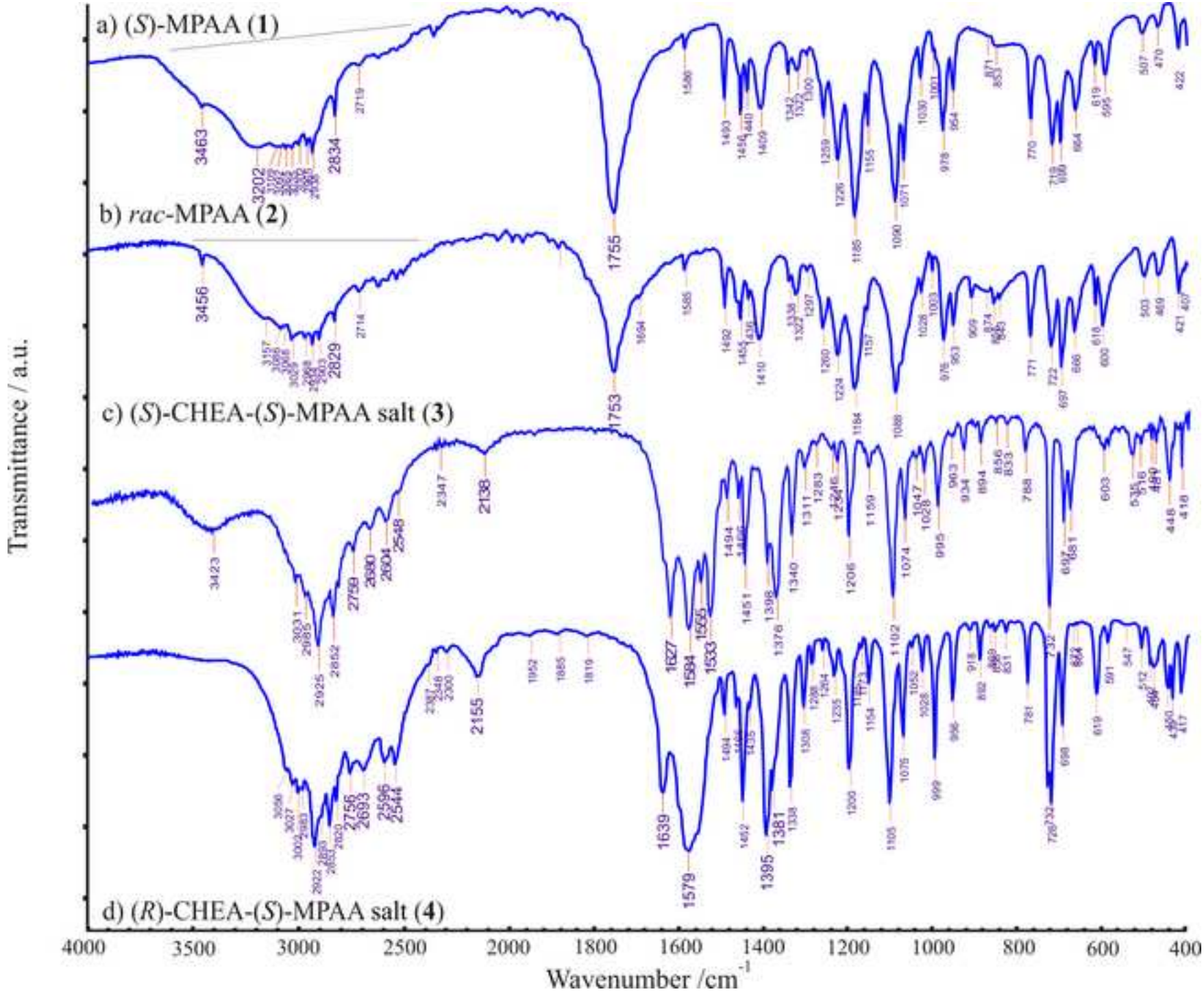

Figure 6

Click here to download high resolution image

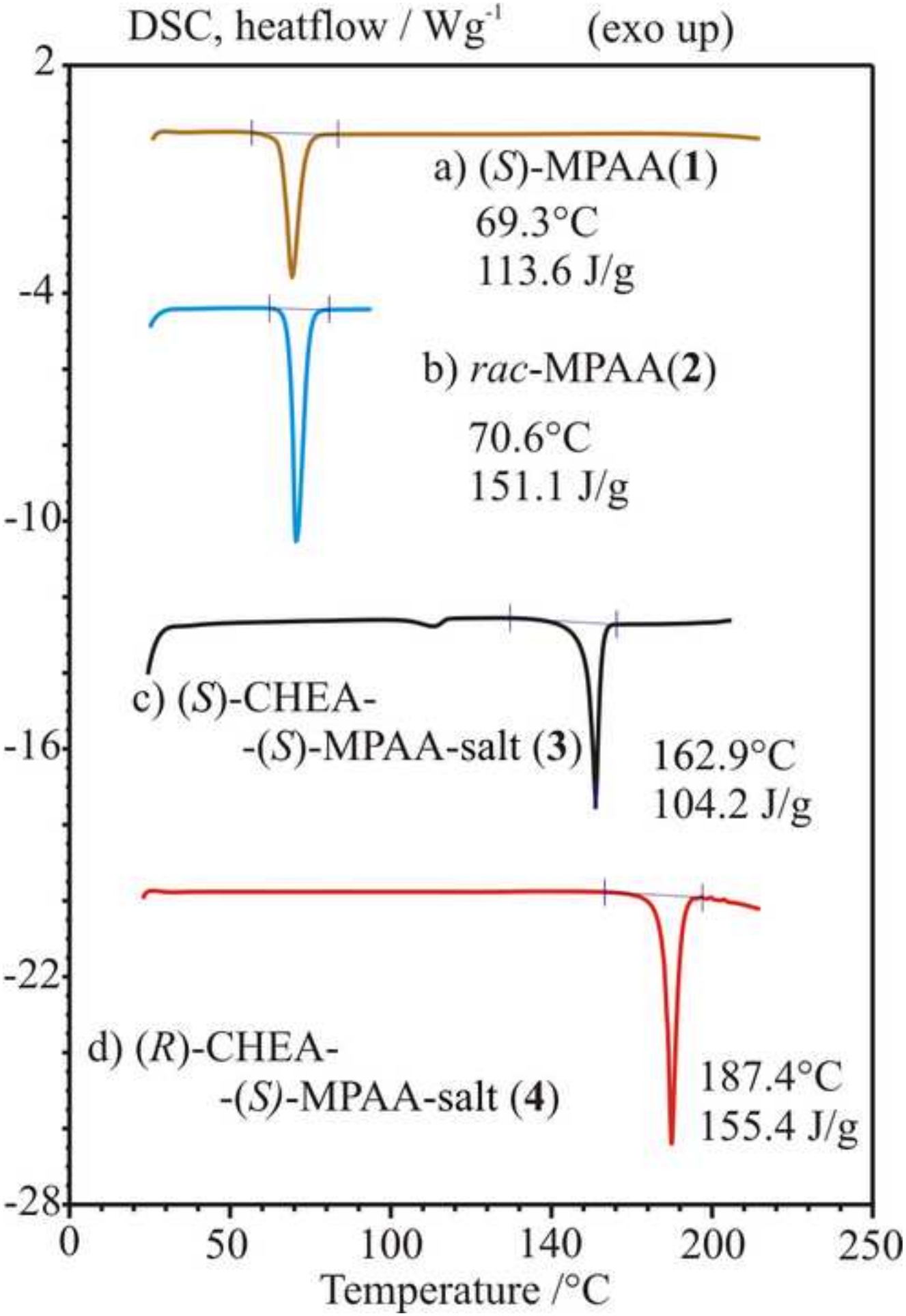

Figure 7

Click here to download high resolution image

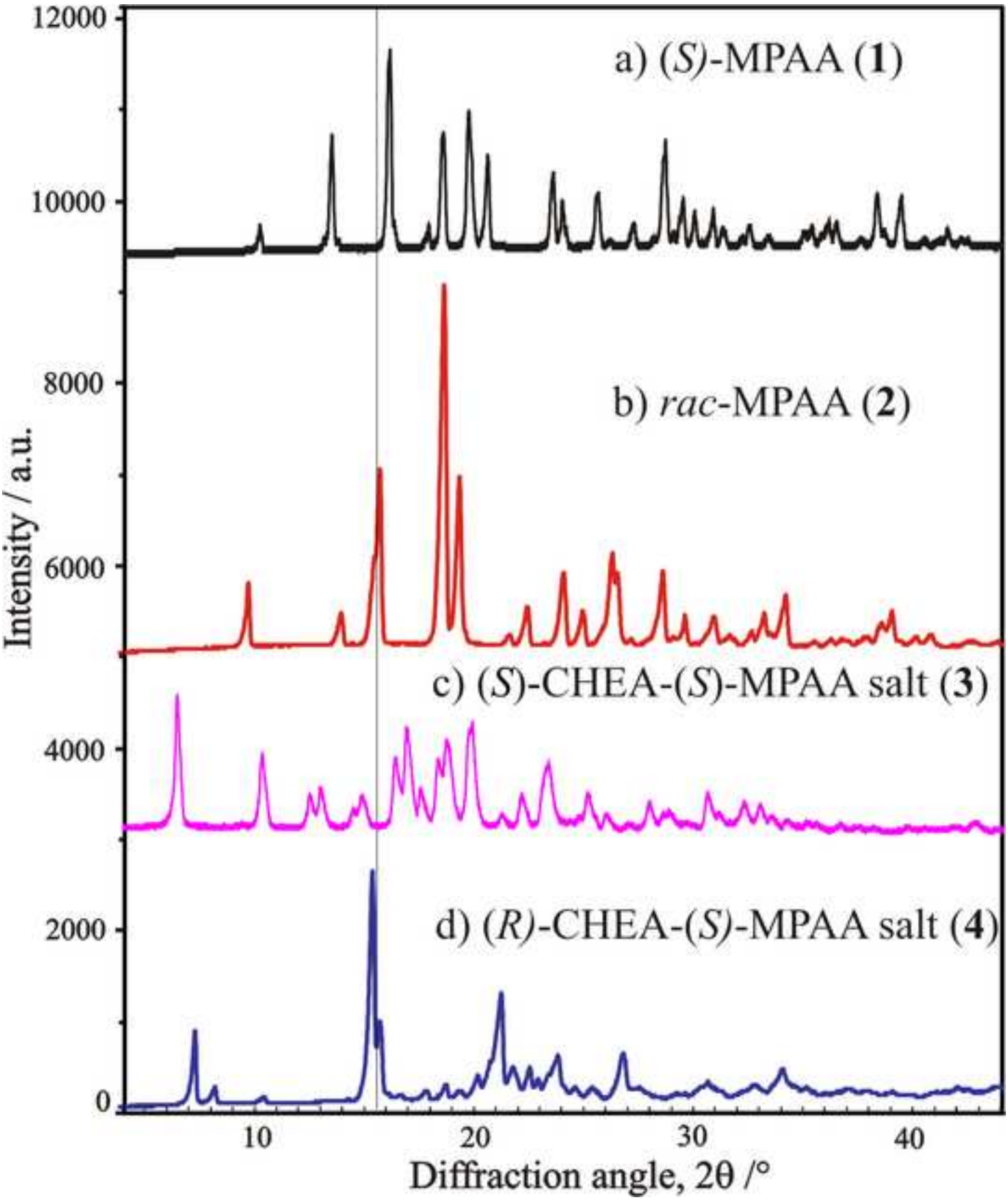

Figure 8

Click here to download high resolution image

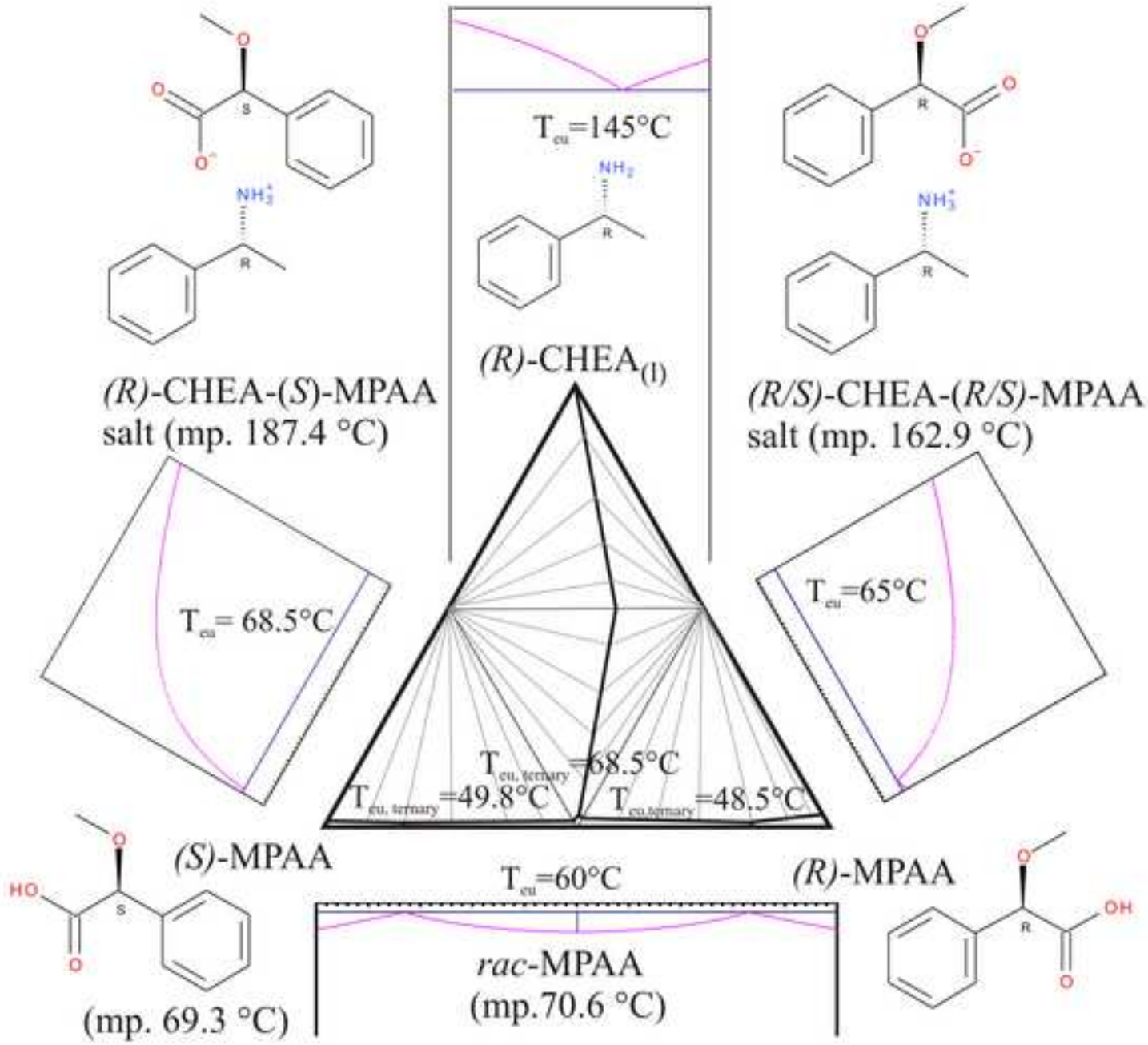

Supplementary Material

Click here to download Supplementary Material: Supplementary Figures and Tables.docx